

## A Mixed-Valent, Fe(II)Fe(I), Diiron Complex Reproduces the Unique Rotated State of the [FeFe]Hydrogenase Active Site

Tianbiao Liu and Marcetta Y. Darensbourg\*

Department of Chemistry, Texas A & M University, College Station, Texas 77845

Received March 22, 2007; E-mail: marcetta@mail.chem.tamu.edu

There is an impressive concurrence of the diiron subunit of the six-iron H-cluster in [FeFe]hydrogenase, [FeFe]H<sub>2</sub>ase, **A**, with a classic Fe<sup>I</sup>Fe<sup>I</sup> organometallic, ( $\mu$ -pdt)[Fe(CO)<sub>3</sub>]<sub>2</sub> (pdt = propane dithiolate, <sup>-</sup>S(CH<sub>2</sub>)<sub>3</sub>S<sup>-</sup>), **B**.<sup>1,2</sup> In the protein crystal structure of the “as isolated” enzyme, the 2Fe site is currently presumed to be in a mixed-valent Fe<sup>I</sup>Fe<sup>II</sup> redox level;<sup>3–5</sup> however, exact Fe oxidation states under various conditions remain ambiguous.<sup>6</sup> From the structures of **A** and **B** in Scheme 1, significant discrepancies are obvious, including, in **A**, the apparent open site on an otherwise octahedral iron and the CO group that toggles between bridging or semi-bridging, dependent on the redox level of the enzyme active site (eas) or adjacent 4Fe4S clusters. The ease of manipulation of complex **B** has led to extensive efforts in the synthesis of derivatives aiming to reproduce structural and spectroscopic features of the eas and to exploit the models for electrocatalysis.<sup>7–9</sup>

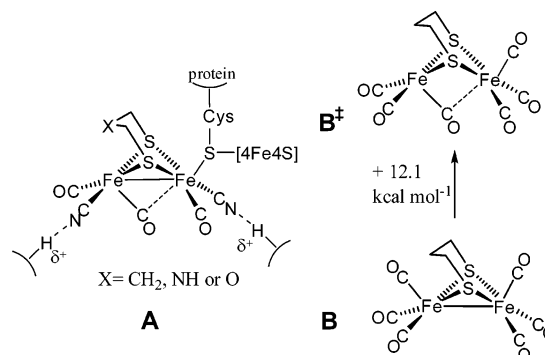
Steady progress made since the definitive report of the H-cluster structure has called upon fundamental principles of organometallic chemistry to guide designs of small molecule analogues with first coordination sphere ligands taking the place of the elaborate protein scaffold.<sup>8</sup> Still there is great difficulty in stabilizing a synthetic analogue with the entatic state or “rotated” structure, **B**<sup>†</sup>, which is computed to exist only as the transition state in CO site exchange processes of ( $\mu$ -SRS)[Fe<sup>I</sup>(CO)<sub>3</sub>]<sub>2</sub>.<sup>10</sup> Furthermore, examples of the mixed-valent Fe<sup>II</sup>Fe<sup>I</sup> state that is observed as a prominent redox level in the enzyme are rare.<sup>6,9</sup>

We and others have explored the possibility that the unique properties of N-heterocyclic carbene (NHC) ligands, such as IMes, 1,3-bis(2,4,6-trimethylphenyl)imidazol-2-ylidene, in ( $\mu$ -pdt)[Fe(CO)<sub>3</sub>][Fe(CO)<sub>2</sub>(IMes)], complex **C**, might be useful in the preparation of Fe<sup>I</sup>Fe<sup>I</sup> electrocatalysts for H<sub>2</sub> production.<sup>11,12</sup> In the course of extending the redox activity of NHC complexes into the H<sub>2</sub> uptake and oxidation regime, we have prepared the unsymmetric disubstituted derivative ( $\mu$ -pdt)[Fe(CO)<sub>2</sub>(PMe<sub>3</sub>)] [Fe(CO)<sub>2</sub>(IMes)], complex **D**. Its fully reversible Fe<sup>I</sup>Fe<sup>I</sup> ⇌ Fe<sup>I</sup>Fe<sup>II</sup> couple has inspired efforts to isolate the mixed-valent complex as a biomimetic whose characterization is the basis of this report. Notably, a remarkable reorientation of the IMes–NHC ligand enables the ( $\mu$ -pdt)[Fe(CO)<sub>2</sub>(PMe<sub>3</sub>)] [Fe(CO)<sub>2</sub>(IMes)]<sup>+</sup> cation, **D**<sub>ox</sub>, to exist as a rotated structure, complete with semi-bridging CO and a protected open site with great structural similarity to the diiron unit of H<sub>as isolated</sub> or H<sub>ox</sub>.

Complex **C** reacts with excess PMe<sub>3</sub> in refluxing toluene, affording complex **D** as a red solid in high purity and yield (see Supporting Information). The four-band  $\nu$ (CO) (Figure 1, blue line, 1972 (s), 1933 (vs), 1897 (s), 1882 (sh)) pattern is consistent with the composition and C<sub>1</sub> symmetry of **D**. The increase in electron density at iron upon introduction of the PMe<sub>3</sub> ligand is indicated by  $\nu$ (CO) IR values lowered by ca. 40 cm<sup>-1</sup> from those of **C**.<sup>11</sup>

The cyclic voltammogram of complex **D** in CH<sub>3</sub>CN shows a fully reversible, one-electron process at –0.47 V (vs Fc<sup>+/0</sup>), assigned as a one-electron oxidation, Fe<sup>I</sup>Fe<sup>I</sup> ⇌ Fe<sup>I</sup>Fe<sup>II</sup>. A second irreversible oxidation (0.14 V) is likely due to further oxidation,

Scheme 1



Fe<sup>I</sup>Fe<sup>II</sup> → Fe<sup>II</sup>Fe<sup>II</sup>. The good reversibility of Fe<sup>I</sup>Fe<sup>I</sup> ⇌ Fe<sup>I</sup>Fe<sup>II</sup> in the electrochemical cell and the separation of this couple from the next redox event suggested a stable Fe<sup>I</sup>Fe<sup>II</sup> species might be isolable from bulk chemical oxidation. Accordingly, ferrocenium was chosen for such purpose, and the Cp\*<sub>2</sub>Co reductant (–1.91 V vs Fc<sup>+/0</sup>/Fc) was used for the reverse process.

Under Ar and at –70 °C in CH<sub>2</sub>Cl<sub>2</sub> solvent, selected for its low coordination ability and to avoid the Fe<sup>II</sup>Fe<sup>II</sup> species,<sup>13</sup> the mixing of **D** with an equivalent of Fc<sup>+</sup>PF<sub>6</sub><sup>-</sup> immediately led to a color change of the solution from dark red to dark brown. An infrared spectral monitor demonstrated that all of **D** converted to a new species, as featured in Figure 1 (red line), with change of  $\nu$ (CO) IR pattern and shifted to higher frequencies representing three CO ligands (2036(s), 1997 (s), 1987 (s, sh)). A less intense band at 1861 cm<sup>-1</sup> is indicative of a bridged or semi-bridged CO group. The terminal CO absorptions are on average ca. 60 cm<sup>-1</sup> blue shifted from those of **D**, consistent with formation of cationic **D**<sub>ox</sub>. That the oxidation process is chemically reversible was shown by treating the **D**<sub>ox</sub> solution with 1 equiv of Cp\*<sub>2</sub>Co (Figure 1, brown line). After reduction, the reaction solution returned to the original dark red color and the IR monitor confirmed both the oxidation and the reduction processes are ~100% efficient. The [**D**<sub>ox</sub>]<sup>+</sup>PF<sub>6</sub><sup>-</sup>

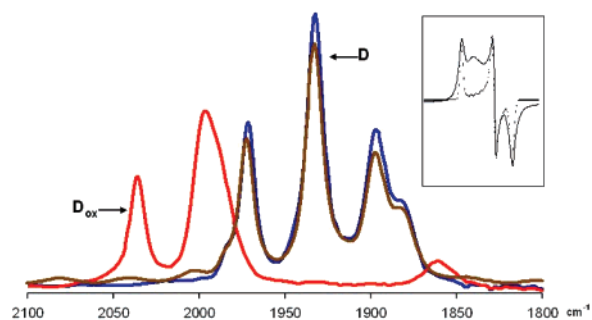
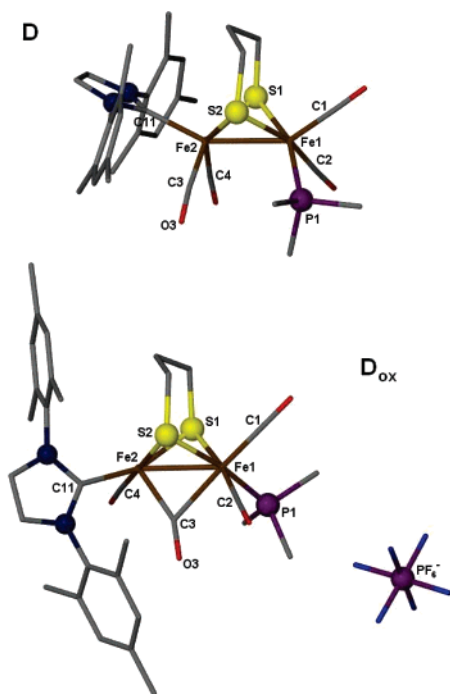


Figure 1. Infrared spectra (CH<sub>2</sub>Cl<sub>2</sub> solution) of complexes **D**<sub>ox</sub> (red line) and **D** (blue and brown lines), showing reversibility of the **D**–**D**<sub>ox</sub> redox pair. The EPR spectrum of **D**<sub>ox</sub> is in the inset (solid line: experimental, dotted: simulated; see text and Supporting Information for details).



**Figure 2.** Molecular structures of complex **D** (top) and complex **D<sub>ox</sub>** (bottom) as ball and stick drawings. Salient metric parameters, **D**, **D<sub>ox</sub>** in italics: Fe(1)–Fe(2) 2.553(2), 2.566(1) Å; Fe(1)–P(1) 2.225(3), 2.268(2) Å; Fe(2)–C(11) 2.013(1), 2.000(4) Å; Fe(1)–C(3) not available for **D**, 2.194(4) Å; Fe(2)–C(3) 1.740(1), 1.864(4) Å; Fe(2)–S(1) 2.276(3), 2.299(2) Å; Fe(2)–S(2) 2.295(3), 2.282(1) Å; S(1)–Fe(2)–C(11) 105.2(3), 160.9(1)°; S(2)–Fe(2)–C(11) 106.9(3), 92.3(1)°; Fe(1)–S(1)–Fe(2) 68.4(1), 68.2(3)°; Fe(1)–C(3)–Fe(2) not available for **D**, 77.9(1)°; Fe(1)–C(3)–O(3) not available for **D**, 129.8(3)°; Fe(2)–C(3)–O(3) not available for **D**, 151.9(3)°.

salt was isolated and crystallized at  $-40$  °C. The  $\nu(\text{CO})$  IR pattern of **D<sub>ox</sub>** is a reasonable match of various reported  $\text{H}_{\text{as isolated}}$  and  $\text{H}_{\text{ox}}$  states of the active site of the  $[\text{FeFe}]\text{H}_2\text{ase}$ .<sup>6</sup> The CO band positions of the (presumed)  $\text{Fe}^{\text{II}}\text{Fe}^{\text{I}}$  redox level  $\text{H}_{\text{ox}}$  from *Desulfovibrio desulfuricans* (2007(s), 1983(vs) and 1848(w)  $\text{cm}^{-1}$ ) are closest to our model complex.<sup>6</sup>

The X-band EPR spectrum (Figures 1 and S3) of brown, paramagnetic  $[\text{D}_{\text{ox}}]\text{PF}_6^-$  is characterized by almost ideal rhombic symmetry with principal  $g$  values simulated to 2.180, 2.096, and 2.052. A minor species with a feature at 2.14 is also evident. The main three  $g$  values are similar to those of  $\text{H}_{\text{ox}}$  ( $g_1 = 2.097$ ,  $g_2 = 2.039$ ,  $g_3 = 1.999$ ).<sup>14</sup> An earlier example of an  $\text{Fe}^{\text{II}}\text{Fe}^{\text{I}}$  model complex, observed in spectroelectrochemical studies at low temperatures, displayed a similar EPR spectrum.<sup>5</sup>

Ball and stick representations of the molecular structures of **D** and **D<sub>ox</sub>** are given in Figure 2, and selected metric parameters are listed in the caption. While the structure of **D** is practically the same as complex **C**,<sup>11</sup> **D<sub>ox</sub>** has undergone a substantial conformational change at the IMes-substituted iron. The  $\text{Fe}(\text{CO})_2(\text{IMes})$  unit has rotated to produce an inverted square pyramid, S-bridged to the  $\text{Fe}(\text{CO})_2\text{PMe}_3$  unit which remains in its original position. The rotation proceeds with placement of one CO underneath the Fe–Fe vector, resulting in a semi-bridging CO group. The asymmetry in the  $\mu$ -CO is evident from the Fe(1)–C(3) and Fe(2)–C(3) distances of 2.196 and 1.864 Å, respectively, and Fe(2)–C(3)–O(3) and the Fe(1)–C(3)–O(3) angles of 151.9(3) and 129.8(3)°, respectively. The IMes ligand has shifted from an apical position

in **D** to a basal position in the inverted square pyramid of **D<sub>ox</sub>** with near eclipse of the NHC plane with the trans Fe–S(1) bond vector. Inspection of the structure of **D<sub>ox</sub>** by space-filling models (Figure S4) finds that the hydrogens of the bridgehead carbon in the iron dithiacyclohexane ring are positioned over the open site and about the face of the arene of the IMes ligand. Thus, in both **D** and **D<sub>ox</sub>**, the orientation of the IMes ligand is so as to avoid stereocongestion with the carbonyl ligands. Consequently, one of the arenes of the NHC in **D<sub>ox</sub>** is ideally positioned to protect or block the open site of Fe(2).

In summary, we have synthesized a stable  $\text{Fe}^{\text{II}}\text{Fe}^{\text{I}}$  paramagnetic  $\text{H}_2\text{ase}$  model complex with semi-bridging CO that well models the  $2\text{Fe}_2\text{S}$ , mixed valent, subsite of the H-cluster in  $[\text{FeFe}]\text{H}_2\text{ase}$ . During the review of this submission a second complex was reported.<sup>15</sup>

Our **D<sub>ox</sub>** model demonstrates the EPR spectral features of a mixed-valent  $\text{Fe}^{\text{II}}\text{Fe}^{\text{I}}$  species which is apparently present both in the  $\text{H}_{\text{as isolated}}$  cluster and in  $\text{H}_{\text{ox}}$ . While the simplicity of our EPR spectrum is similar to some forms of  $[\text{FeFe}]\text{H}_2\text{ase}$ , complications are present in others where the redox level of  $4\text{Fe}_4\text{S}$  clusters permits their involvement. Preliminary computational results suggest the unpaired spin density and the SOMO are on the rotated iron, that is, the  $\text{Fe}^{\text{I}}$ .<sup>16</sup> Thus, the “open site” in the mixed-valent, resting form of the enzyme is poised to be readily activated by redox changes to perform both hydrogenase functions,  $\text{H}^+$  reduction, and  $\text{H}_2$  binding and oxidation.

**Acknowledgment.** We acknowledge financial support from the National Science Foundation (CHE-0616695 to M.Y.D.) and the R.A. Welch Foundation (A-0924). We also thank the X-ray crystallography facility and Dr. Joe Reibenspies.

**Supporting Information Available:** Full structure files; complete description of experiments; cyclic voltammograms and EPR spectra. This material is available free of charge via the Internet at <http://pubs.acs.org>.

## References

- (1) Nicolet, Y.; Lemon, B. J.; Fontecilla-Camps, J. C.; Peters, J. W. *Trends Biochem. Sci.* **2000**, *25*, 138–143.
- (2) Darensbourg, M. Y.; Lyon, E. J.; Zhao, X.; Georgakaki, I. P. *Proc. Natl. Acad. Sci. U.S.A.* **2003**, *3683*–3688.
- (3) Popescu, C. V.; Münck, E. *J. Am. Chem. Soc.* **1999**, *121*, 7877–7884.
- (4) Nicolet, Y.; de Lacey, A. L.; Vermede, X.; Fernandez, V. M.; Hatchikian, E. C.; Fontecilla-Camp, J. C. *J. Am. Chem. Soc.* **2001**, *123*, 1596–1601.
- (5) Razavet, M.; Borg, S. J.; George, S. J.; Best, S. P.; Fairhurst, S. A.; Pickett, C. J. *Chem. Commun.* **2002**, 700–701.
- (6) Roseboom, W.; de Lacey, A. L.; Fernandez, V. M.; Hatchikian, E. C.; Albracht, S. P. J. *J. Biol. Inorg. Chem.* **2006**, *11*, 102–118.
- (7) Tard, C.; Liu, X. M.; Ibrahim, S. K.; Bruschi, M.; De Gioia, L.; Davies, S. C.; Yang, X.; Wang, L. S.; Sawers, G.; Pickett, C. J. *Nature* **2005**, *433*, 610–613.
- (8) (a) Van der Vlugt, J. I.; Rauchfuss, T. B.; Whaley, C. M.; Wilson, S. R. *J. Am. Chem. Soc.* **2005**, *127*, 16012–16013. (b) Justice, A. K.; Zampella, G.; De Gioia, L.; Rauchfuss, T. B. *Chem. Commun.* **2007**, published online.
- (9) Borg, S. J.; Behrsing, T.; Best, S. P.; Razavet, M.; Liu, X.; Pickett, C. J. *J. Am. Chem. Soc.* **2004**, *126*, 16988–16999.
- (10) Lyon, E. J.; Georgakaki, I. P.; Reibenspies, J. H.; Darensbourg, M. Y. *J. Am. Chem. Soc.* **2001**, *123*, 3268–3278.
- (11) Tye, J. W.; Lee, J.; Wang, H. W.; Mejia-Rodriguez, R.; Reibenspies, J. H.; Hall, M. B.; Darensbourg, M. Y. *Inorg. Chem.* **2005**, *44*, 5550–5552.
- (12) Capon, J. F.; El Hassnaoui, S.; Gloaguen, F.; Schollhammer, P.; Talarmin, J. *Organometallics* **2005**, *24*, 2020–2022.
- (13) Justice, A. K.; Linck, R. C.; Rauchfuss, T. B. *Inorg. Chem.* **2006**, *45*, 2406–2412.
- (14) Bennett, B.; Lemon, B. J.; Peters, J. W. *Biochemistry* **2000**, *39*, 7455–7460.
- (15) Rauchfuss, T. B.; Justice, A. K.; Stanley, J. L. Abstracts INOR-487, 233rd ACS National Meeting, Chicago, IL, March 25–29, 2007.
- (16) Thomas, C. M.; Darensbourg, M. Y.; Hall, M. B. *J. Inorg. Biochem.* Submitted.

JA071851A